Ring-shaped structure in free surface flow of non-Newtonian liquids

Nilesh H. Parmar and Mahesh S. Tirumkudulu
Department of Chemical Engineering, Indian Institute of Technology–Bombay, Powai, Mumbai 400076, India
(Received 26 February 2009; revised manuscript received 5 August 2009; published 3 September 2009)

We report the formation of a ringlike structure in the flow of particular non-Newtonian liquids coating a rotating vertical disk. Experiments were performed with a known volume of the liquid and at varying rotation rates such that the inertial effects were negligible. The liquid injected on the rotating disk initially coats the surface uniformly, which then redistributes itself such that at steady state a significant amount collected into a circular ring, off center with the axis of rotation. Beyond a critical rotation speed and for a given liquid volume, the ring formation did not occur. The ring formation was not observed in the case of Newtonian liquids. Rheological measurements along with the shear rate calculations suggest that the shear thinning nature of the liquids could be responsible for the observed ring formation.

DOI: 10.1103/PhysRevE.80.036303 PACS number(s): 47.57.Qk, 47.50.Cd, 47.55.nd

I. INTRODUCTION

It is well known that non-Newtonian liquids show a diverse range of interesting flow phenomena [1]. Many of the remarkable flow behaviors of polymer melts and solutions such as the rod-climbing phenomenon, convex interface of a polymeric fluid flowing down an open inclined channel, die swelling, tubeless siphon, etc. can be attributed to the elastic nature of the fluid [1,2]. For example, the rod-climbing effect is caused by the hoop stresses generated by the stretched and oriented polymers that push the fluid toward the rod causing the fluid to climb the rod. These unique flow patterns stem from the coupling between the macromolecular structures of the fluid and the flow.

Here, we report a unique flow pattern akin to the aforementioned effects for particular non-Newtonian liquids coating a rotating vertical disk. Here, the disk rotates very slowly so that the viscous liquid that coats the entire vertical disk redistributes under viscous, gravitational, and surface-tension forces. The flow geometry under consideration is somewhat related to the Landau-Levich problem [3] of a plate that is drawn out of a bath and the final film thickness for a Newtonian liquid is determined from a balance of the same three forces. The analogy becomes apparent if we consider a vertical disk of radius R that rotates at an angular velocity Ω. In this case, the viscous force pulling the fluid up scales as $\mu\Omega R/h$ while the downward pull of the gravity goes as $\rho g h$. Here, μ and ρ are the viscosity and the density of the fluid, h is film thickness, and g is the gravity constant. This suggests that, in the absence of surface-tension effects, a liquid film of thickness $h \sim \sqrt{\mu\Omega R/\rho g}$ can be prevented from dripping if the vertical disk is rotated at the given conditions. A closely related problem is that of a viscous liquid coating a horizontal rotating cylinder where Moffatt [4] balanced the gravity and the viscous force under the lubrication approximation to find similar scalings for the film thickness.

Most studies on coating flows on disks have focused on the spin coating flow geometry due its importance in the electronic industry. Here, a *horizontal* disk coated with a liquid rotates at a high speed, so that the liquid film spreads out radially under centrifugal force against the viscous and the surface-tension forces [5,6]. The gravity acts *perpendicular* to the disk while the film thickness profile is axisymmetric. In contrast, the gravity acts parallel to the disk surface for the vertical rotating disk leading to a complicated spatial distribution of the film thickness. Although not studied as extensively, rotating vertical disks find industrial application too such as in a rotating disk reactor where stainless steel disk mounted on a horizontal shaft rotates inside in a cylindrical shell filled partially with liquid [7]. The rotating disk carries a thin film of liquid, which is brought in contact with a gas phase for an enhanced gas-liquid mass transfer. The main advantage of the rotating disk reactor is that the interfacial gas-liquid area is constant and known. Such reactors find extensive applications in polymer processing, biochemical processing involving fermentation, and waste water processing.

In this paper, we focus on detailed experimental results related to the flow behavior of non-Newtonian liquids coating vertical rotating disks. The thickness profiles measured for the Newtonian liquids are distinctly different from those measured for the non-Newtonian liquids. Specifically, the non-Newtonian liquids exhibit a unique flow pattern where a significant fraction of the liquid collects into a circular ring offset from the center of the disk, whereas no such feature is present for the Newtonian liquid. The formation of the ring is found to depend on the numerical value of a dimensionless variable obtained from the balance of the viscous and the gravitational forces. We discuss in detail the measured rheology of the non-Newtonian liquids and conclude with remarks on the possible mechanism for the ring formation.

II. EXPERIMENTS

Figure 1 presents a schematic of the experimental setup. A vertical flat stainless steel disk was attached to a stepper motor, so that the disk could be rotated over a wide range of rotation rates. Varying liquid volumes were selected so that the liquid coated the disk completely with the contact line pinned at the circumference of the disk. The film thickness was measured by contacting a needle with the liquid surface. The needle was placed on an xyz micrometer traverse of least count of 0.01 mm which in turn was placed on an xy traverse with a coarse movement of 100 mm in each direction and a

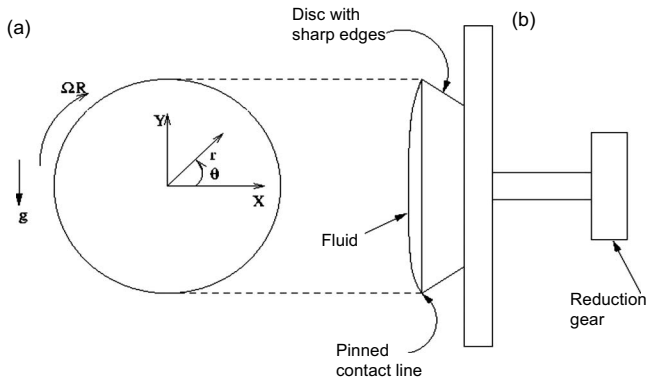

FIG. 1. The schematic of the experimental setup: (a) front view of the rotating disk and (b) side view of the setup.

least count of 1 mm. Since the displacement of the needle when it contacts the disk surface is known from calibration, the difference between that value and the displacement when the needle contacts the film gives the local film thickness.

Since the accuracy of the final measurement depends on the alignment of the traverse with respect to the vertical disk, a detailed calibration was performed prior to the experiments to determine the error in thickness measurement. At a fixed y, the needle was made to contact the disk surface at a number of points along the x direction. This was repeated at various vertical positions (for different y) on the disk surface. The maximum variation in the disk position over the entire surface was found to be less than ± 0.05 mm. Once the average disk surface position (z coordinate of the disk surface) was known, the liquid film thickness profile was determined by noting the z coordinate of the liquid film (the free surface) at various locations on the disk and then subtracting the disk surface position from it.

Experiments were performed with transparent silicone oils (Newtonian) with viscosities of 5 and 35 Pa s and a surface tension of 31 dyn/cm at varying rotation speeds, disk diameters, and liquid volumes. The non-Newtonian liquids included a commercially available shampoo, Sunsilk® (from Unilever PLC) and an equimolar (0.05 M) aqueous solution of cetyl trimethyl ammonium bromide (CTAB) and sodium salicylate (NaSal). The CTAB-NaSal mixture was prepared in de-ionized water and the mixture was left to equilibrate for 3 days before the start of the experiments. The steady shear viscosity and the first normal stress difference for shampoo were measured at 25 and 30 °C on a cone and plate geometry with a cone angle of 0.02 rad and a plate diameter of 50 mm [Fig. 2(a)]. The rheology of the CTAB-NaSal solution was measured using a Couette geometry and was found identical to that reported by Won-Jong and Yang [8], which was measured on an ARES® rheometer using a cone and plate geometry of 50 mm in diameter with the cone angle of 0.04 rad. Figure 2(b) shows the steady shear viscosity of the solution over the measured range of shear rates. Both the liquids show shear thinning behavior over the measured range. Figure 2(a) suggests that the shampoo does not exhibit any significant normal stress differences for shear rates less than 1 s^{-1}. The storage and the loss moduli of the shampoo and the CTAB-NaSal solution are presented in Fig. 3.

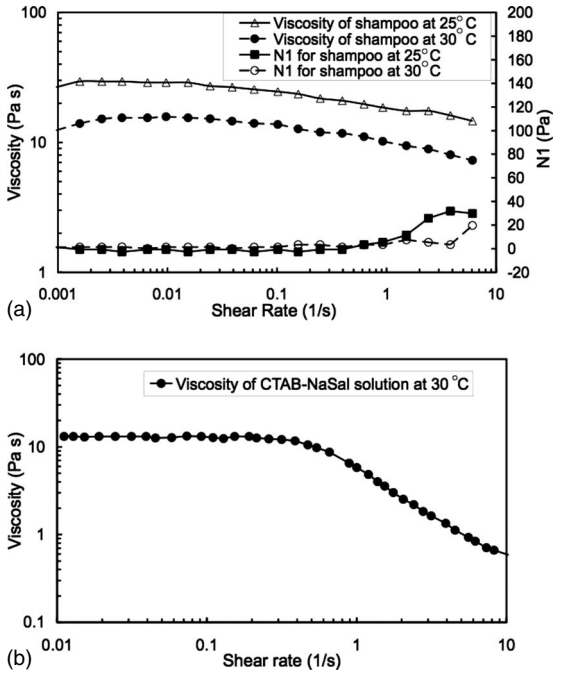

FIG. 2. Steady shear viscosity of (a) shampoo and (b) CTAB-NaSal solution [8] and first normal stress difference (N1) of shampoo measured on a cone and plate geometry.

In all experiments, the disk surface was wet mildly with a moist cloth prior to liquid injection to facilitate easy spreading of the liquid. Detailed experiments were performed with the shampoo on 7- and 9-cm-diameter disks at liquid volumes varying from 3 to 7 ml and rotation rates from 1 to 4

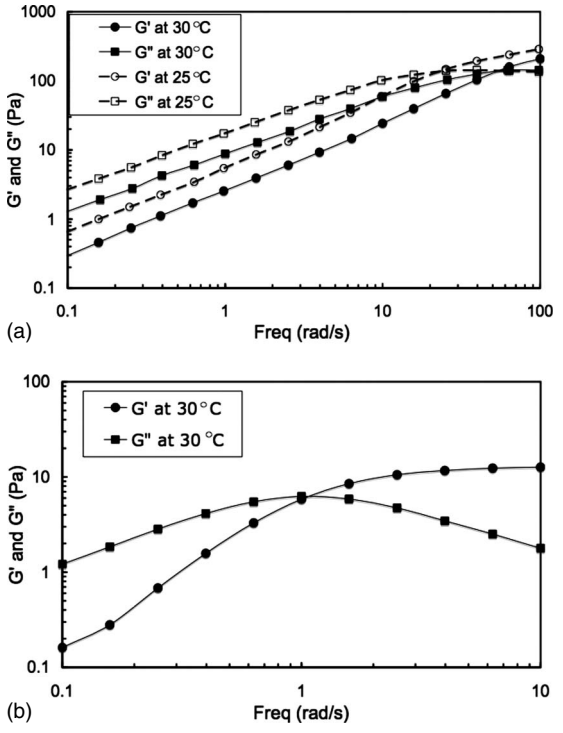

FIG. 3. Small-angle oscillatory shear measurements for (a) shampoo and (b) CTAB-NaSal solution [8].

TABLE I. Summary of fluid properties and experimental parameters.

Liquid	Density (kg/m^3)	Rotation rate (rpm)	Disk diameter (cm)	Volume (ml)	Temperature (°C)
Silicon oils	900	1–4	7, 9	3–6	30
Shampoo	1030	1–4	7, 9	3–7	25, 30
CTAB-NaSal	1100	3–4	7, 9	3–4	30

rpm (Table I). The Reynolds number $\mathrm{Re} \equiv \rho \Omega R h_0 / \mu$ was negligible in all cases. Here, h_0 is the average film thickness. The temperature and the humidity of the room were monitored throughout the experiment and the variation was small (± 0.1 °C and $\pm 1\%$ RH).

Experimental results

1. Newtonian liquids

Film thickness profile was measured at steady state along vertical and horizontal sections of the disk to get a quantitative measure of the thickness variation. The film thickness values were interpolated over the disk surface to get the full film thickness profile. Figure 4 shows the contours of dimensionless heights ($H \equiv h/h_0$) obtained from the interpolated values for an experiment performed on a 7-cm-diameter disk rotating at 2 rpm and coated with 5 ml of silicone oil with a viscosity of 35 Pa s. The height contours appear to be somewhat symmetric about the horizontal diameter with larger thicknesses in the left half of the disk. In fact, the point of maximum height ($H=1.87$) occurs along the horizontal diameter on the left half of the disk. This is because the average liquid velocities are lower for $x<0$ compared to $x>0$ where both the gravity and the viscous force act in the same direction. Thus, for the same volume flux, we would expect thicker films for $x<0$. Further, the thickness decreased monotonically from the peak in all directions. With decreasing rotation rate at a fixed volume, the asymmetry across the vertical diameter (i.e., for y constant) was found to increase implying that more liquid is accumulated in $x<0$. As a check on the accuracy of the measurement system, the liquid volume was calculated for the Newtonian case by integrating the measured thickness profile and was found to differ by less than 3% from the disbursed volume.

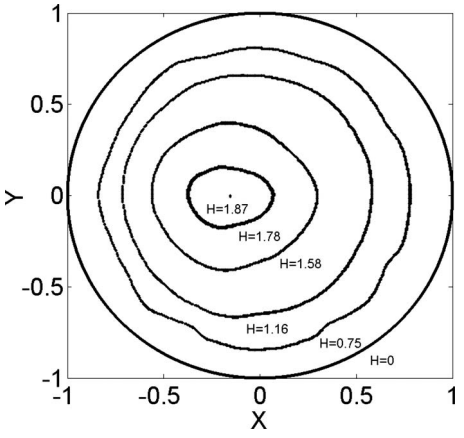

FIG. 4. Constant height contours on a 7-cm-diameter circular disk rotating clockwise at 2 rpm and coated with 5 ml of silicone oil with a viscosity of 35 Pa s. The x and the y coordinates are nondimensionalized by the disk radius while the thickness is rendered dimensionless by the average film thickness.

2. Non-Newtonian liquids

We next present results of experiments conducted with the non-Newtonian liquids. Photographs in Fig. 5 show the dynamics of ring formation for 6 ml of shampoo on a 9-cm-diameter disk rotating at 2 rpm in the clockwise direction. Here, photographs are shown after 2, 3, 4, and 7 min of complete injection of liquid on the rotating disk. It can be seen from the figure that the liquid starts collecting on the left half of the disk and forms a faint ringlike structure within 2–3 min of the start of the experiment. A small blob of liquid appears close to the periphery of the disk on the left half of the ring. After 7 min, the flow reaches steady state with the ring becoming distinct. It is important to note that the position of the ring (and the blob) does not change in the laboratory frame of reference. Ring formation was observed with both diameter disks.

A similar set of ring formation images of the CTAB-NaSal mixture is presented in Fig. 6. These images have been taken along the disk surface so as to highlight the dynamics of the free surface. Within 1 min of applying the

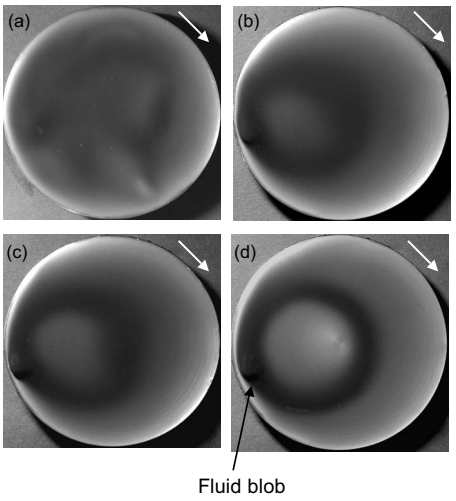

FIG. 5. Dynamics of ring formation for 6 ml of shampoo coating a 9-cm-diameter disk rotating at 2 rpm (a) at the start and after (b) 2, (c) 3, and (d) 7 min. The ambient temperature was 30 °C. The white arrows show the direction of rotation.

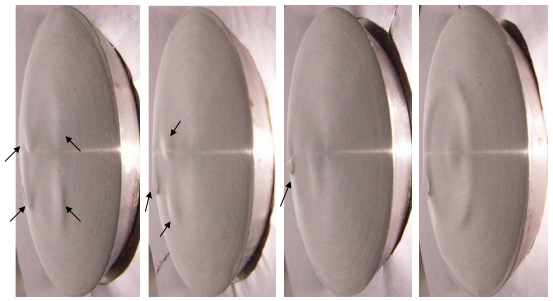

FIG. 6. (Color online) Formation of the ring: (a) small teardrops after 1 min, (b) the drops after 3 min, (c) merging of the drops into a single blob after 5 min, and (d) formation of ring after 6 min for 3.5 ml of CTAB-NaSal mixture on the 9-cm-diameter disk rotated at 4 rpm. The drops are highlighted by arrows. The ambient temperature was 30 °C.

liquid, three to four hanging drops (or blobs) moved over the disk as the latter rotated. This continued for about 5 min, after which they merged and formed a single (larger) blob. This blob was not stationary but moved with the disk while disappearing and reappearing at different regions of the disk. This process continued for about 1 min after which the position of the blob remained steady at the left edge of the disk. Soon a ring appeared and it remained steady. It was easier to detect the presence of a ring with the shampoo due to its black color compared to the transparent solution of the CTAB-NaSal mixture.

As mentioned previously, the formation of the blob was always preceded by the formation of a single large blob on the left side of the disk. To determine if the formation of the ring depended on the initial condition, we disturbed the ring with a needle. The liquid in the ring mixed with the surrounding liquid and the ring disappeared. However, within a few minutes, a single large blob formed from smaller blobs followed by the formation of the ring. The process of formation took longer for higher rotation rates. We also disturbed the flow by withdrawing a small amount of liquid from the final blob in the presence of the ring. The ring disappeared but reappeared after the blob reformed at the left edge of the disk. This process was repeated a few times and the formation of the ring was always preceded by the stabilization of the blob on the left side of the disk. Finally, when sufficient liquid had been removed from the large blob, smaller blobs (around two to three) appeared which did not coalesce but could be seen moving on the left half of the rotating disk. No steady state was reached in such cases. During this time, no significant (visual) change in film thickness was observed on the right side of the disk. These experiments suggest that, for a fixed rotation rate, there is a minimum volume below which the ring does not form.

We also investigated if the presence of the ring also requires the presence of the blob. In other words, is a blob always present when a ring is present? Although it was observed that a single blob must form before the ring formation, the size of the final blob in the presence of the ring was variable. Figure 7 shows the ring at steady state where a blob is visible for the larger volume (4 ml) but seems to be absent for 3 ml (h_0=0.47 mm).

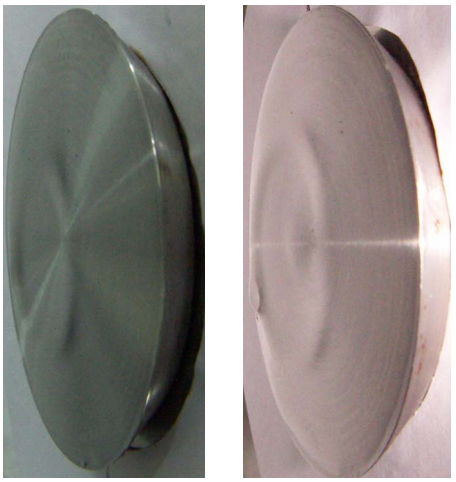

FIG. 7. (Color online) Ring formation for CTAB-NaSal solution for (a) 3 and (b) 4 ml, for the 7 cm disk rotating at 4 rpm. The ambient temperature was 30 °C.

Given the ease of detecting the ring in the shampoo, we performed many experiments with this fluid. Experiments performed at different rotation rates (1–3 rpm) on the 9-cm-diameter disk for a given liquid volume showed that the location of the ring was the same irrespective of the rotation rates although the ring appeared diffuse with increasing rotation rate. Experiments were also performed at a fixed rotation rate (1 rpm) with varying liquid volumes on the 9-cm-diameter disk. The ring appeared more distinct for higher volumes (5 and 6 ml) than at the lower volume (4 ml). Here, too, experiments conducted over a range of rotation speeds and liquid volumes suggest that for a given disk diameter and rotation speed there exists a critical volume below which the ring is not formed. For example, no ring was formed when the 9-cm-diameter disk rotating at 1 rpm was coated with liquid volumes less than 4 ml. In this case, several blobs moved over the rotating disk and the flow did not reach steady state. Also, beyond a critical rotation speed and for a given liquid volume, the ring formation did not occur. For example, for the 9-cm-diameter disk at rotation rates greater then 4 rpm, no ring was formed for the case of the shampoo. Here again, no steady state was reached. In all experiments with the shampoo, like with CTAB-NaSal solution, fluid blob always preceded the formation of the ring.

While the ring formation in the case of the shampoo and the CTAB-NaSal mixture was robust and steady, drying could affect the profile after about 1 h when the setup was exposed to the ambient conditions. Consequently, reliable film thickness measurements could only be done along one of the axes in a given experiment. Figure 8(a) shows the nondimensional film thickness (H) profile, rendered dimensionless by the average film thickness (h_0=0.078 cm), along y=0 for a shampoo experiment (at 30 °C) performed on a 7-cm-diameter disk rotating clockwise at 1 rpm for 5 ml of shampoo volume. The plot shows a steep variation in the film thickness values on the left half of the disk where it rises sharply from $H(x=-1)=0$ to a maximum value $H(x=-0.75)=2.30$. The thickness next falls equally rapidly to

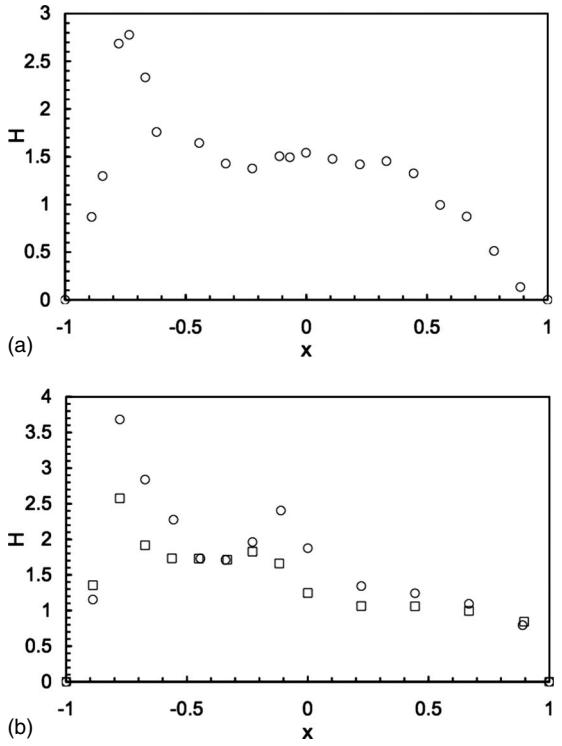

FIG. 8. Measured nondimensional film thickness profile for (a) shampoo (at 30 °C) on a 7-cm-diameter disk along $y=0$ at 1 rpm for 5 ml of volume and (b) CTAB-NaSal (at 30 °C) on a 7-cm-diameter disk along $y=0$ for 3 ml liquid volume at 3 (○) and 4 rpm (□).

$H=1.75$ at $x=-0.6$ followed by a more gradual decrease to $H=1.4$ at $x=-0.2$, which is the center of the ring. For higher values of x, the film thickness again increases to $H=1.5$ at $x=0$ and then decreases monotonically to $H=0$ at $x=1$. A comparison of the measured thickness profile with that of the Newtonian case (Fig. 4) for $y=0$ clearly elucidates the difference in the two profiles for $x<0$.

Figure 8(b) shows the nondimensional film thickness (H) profiles, rendered dimensionless by the average film thickness ($h_0=0.078$ cm) along $y=0$ for the CTAB-NaSal experiments (at 30 °C) performed on a 7-cm-diameter disk coating 3 ml of liquid volume rotating at 3 and 4 rpm. In this case also, the plot shows a steep variation in the film thickness values on the left half of the disk where it rises sharply from $H(x=-1)=0$ to a maximum value $H(x=-0.77)=3.68$ for 3 rpm and $H(x=-0.77)=2.58$ for 4 rpm. It should be noted that the location of the maximum thickness which corresponds to the liquid blob position on the disk surface for both the rotation rates is identical at $x=-0.77$, $y=0$. The thickness next falls rapidly to $H=1.71$ at $x=-0.34$ for both the rotation rates and then increases to $H=2.4$ at $x=-0.11$ for 3 rpm and $H=1.83$ at $x=-0.23$ for 4 rpm. After $x=0.2$ the film thickness decreases gradually for both the rotation rates. The influence of rotation rate on the ring formation is evident here as the spatial variation of thickness is larger at the lower rotation rate. The position of the center of the ring, however, does not change. These measurements confirm the earlier observation with the shampoo where the ring position did not change with the rotation rate.

Since the shampoo and the CTAB-NaSal mixture are both water-based solutions, experiments were repeated with the disk enclosed inside an acrylic cylinder to eliminate drying effects. Here, too, the liquid collected into a ring confirming the absence of drying effects on the flow. Interestingly, the flow could be switched from the "ring" state to the "no ring" state (and back) by changing the ambient temperature during the course of the experiment. For example, the ring disappeared when the ambient temperature was reduced from 30 to 25 °C for the 9-cm-diameter disk rotating at 1 rpm and supporting 6 ml of shampoo. The ring reappeared when the temperature was raised back to 30 °C. This reconfirms the absence of drying effects on the ring formation and suggests that the phenomenon is sensitive to small changes in the rheology of the liquid.

The small-angle oscillatory shear measurements presented in Figs. 3(a) and 3(b) give a measure of the elasticity of the material with the characteristic relaxation time, which is roughly the longest time required for the elastic structures in the liquid to relax, obtained from the inverse of the crossover frequency. In the case of shampoo [Fig. 3(a)], the relaxation times of 0.045 and 0.018 s at 25 and 30 °C, respectively, are more than two orders lower than the typical flow time scale (Ω^{-1}) and about an order of magnitude smaller than the reciprocal of the characteristic shear rate, $h_0/\Omega R$. In the case of CTAB-NaSal solution [Fig. 3(b)], the relaxation time (1 s) at 30 °C is comparable with the typical flow time scale. Thus, not only is the ring formation phenomenon observed over a wide range of relaxation times, it appears also when the relaxation time is small compared to the flow time scale, implying that the elasticity of the fluid may not be contributing to the ring formation.

We also do not expect normal stress differences to cause the ring formation since otherwise the hoop stress generated by the circular streamlines in the left half of the disk would collect more liquid in that region rather than deplete it of fluid. Also, the normal stress difference is negligible for the expected range of shear rates (<1 s^{-1}). Further, stress ramp experiments performed on shampoo at 25 and 30 °C on the cone and plate geometry showed a gradual decrease in the viscosity, which suggests the absence of yield stress in the shampoo.

As both the test liquids are shear thinning fluids, it may be instructive to evaluate the shear field on the disk surface to get an insight into the ring formation phenomenon. In the limit of lubrication approximation and in the absence of surface tension effects, the dimensionless velocity gradients in the Cartesian coordinates for a *Newtonian* liquid are given by

$$\frac{\partial u_x}{\partial z}=0, \quad \frac{\partial u_y}{\partial z}=\alpha(z-H).$$

Here, α is the ratio of the gravitational to the viscous force; $\alpha \equiv \rho g h_0^2/(\mu \Omega R)$; x and y are coordinates in the plane of the disk and rendered dimensionless by R; z is nondimensionalized by h_0; and u_x and u_y, which correspond, respectively, to the fluid velocities in the x and the y directions, are rendered dimensionless by ΩR. The shear field for a Newtonian liquid can then be approximated by

$$\dot{\gamma} = \sqrt{\frac{1}{2}\left[\left(\frac{\partial u_x}{\partial z}\right)^2 + \left(\frac{\partial u_y}{\partial z}\right)^2\right]} = \frac{\alpha}{\sqrt{2}}[H(x,y) - z]. \quad (1)$$

Equation (1) shows that, for a given thickness profile, the shear rate increases with α. Further, for fixed values of α and z, regions of large film thicknesses will have higher shear rates. Based on the above relation and the rheological measurements, it appears that the ring formation could be a consequence of the shear thinning property of the liquid. For the clockwise rotation of disk, majority of the liquid collects on the left half of the disk where the gravitational and the viscous forces oppose each other. While the liquid close to the disk gets carried over from the left half to the right half of the disk, the liquid close to the liquid-air interface (or away from the disk surface) falls back on the left side resulting in recirculation and consequently in higher shear rates. This is further supported by Eq. (1) where the large film thickness on the left side of the disk (for clockwise rotation) leads to high shear rates in those regions. This could cause a reduction in liquid viscosity leading to the depletion of liquid from the recirculating regions and the formation of the ring-shaped structure. The proposed mechanism is supported by experiments where an increased rotation rate at a fixed volume and a decreased liquid volume at a fixed rotation rate lead to diffused rings.

To correlate the results of the shampoo experiments with the proposed mechanism, we calculated the value of α for a power-law fluid whose shear stress is given by

$$\tau_{ij} = 2mE^{n-1}\dot{\gamma}_{ij}. \quad (2)$$

Here, E is the second invariant of the rate of deformation tensor and $\dot{\gamma}_{ij}$ is the shear rate tensor. If we assume that the film is thin compared to the disk radius, $h_0 \ll R$, and if the pressure scaling is set as $(m\Omega R^2/h_0^2)(h_0/\Omega R)^{1-n}$, then the equivalent α for a power-law liquid is given by

$$\alpha = \frac{h_0^2}{m\Omega R}\left(\frac{h_0}{\Omega R}\right)^{n-1}\rho g. \quad (3)$$

Here, the coefficient m and the exponent n were obtained from the curve fits in Fig. 9(a). Since the viscosity does not vary significantly for shear rates less than 0.1 s^{-1}, we only considered points above this value for the curve fit. Figure 9(b) plots the average film thickness as a function of α for experiments performed with shampoo on 7- and 9-cm-diameter disks at 25 and 30 °C. Here, the closed symbols represent the experiments where ring formation was observed while the open symbols represent those without ring formation. It is clear from the figure that for a given temperature there is a critical value of α above which the ring formation was present. This is in agreement with our earlier observation of a minimum liquid volume and a maximum rotation speed for the ring formation. At 30 °C, the critical α is ~0.09, while at 25 °C it is ~0.18. Further, it should be recalled that the flow could be switched from the ring state to the no ring state by decreasing the ambient temperature. This observation is also in line with the above analysis since the ring formed for the 9-cm-diameter disk rotating at 1 rpm and supporting 6 ml of shampoo (h_0=0.095 cm) with the corresponding value of α at 30 °C being 0.24. But on decreasing the temperature to 25 °C, for which the α reduces to 0.14, the ring disappeared.

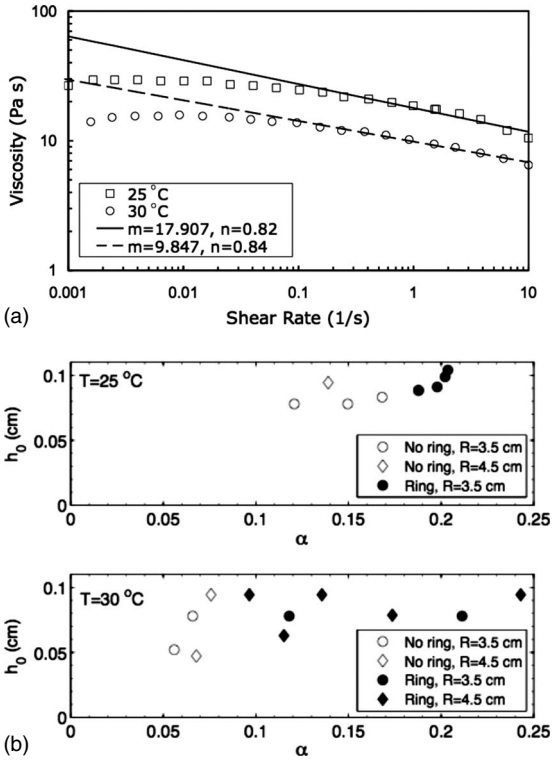

FIG. 9. (a) Power-law fit for the shampoo rheology and (b) regimes of ring formation for varying α corresponding to experiments with varying disk diameters, rotation rates, and volumes of the shampoo at 25 and 30 °C.

We expected the critical α for ring formation to be independent of temperature and the possible variation could be due to the shape of the viscosity versus the shear rate profile for the shampoo. Specifically, the viscosity is constant at both temperatures for shear rates below 0.1 s^{-1}. Thus, one may not expect ring formation at low values of α, which corresponds to the Newtonian case.

Given these results, we were motivated to perform a lubrication analysis to predict the film thickness profile. We solved numerically the film evolution equation including the surface tension term and found an excellent match with experiments in the case of Newtonian liquids.[1] However, on using an Ellis model that fit the shear thinning rheology for the entire range of shear rates for the shampoo and the CTAB-NaSal solution, we were unable to predict the ring. Specifically, the predicted profile was qualitatively similar to that obtained for the Newtonian liquids, i.e., the profile had a maximum along $y=0$, $x<0$ from where the thickness decreased monotonically toward the disk edge. Further, with increasing α, the location of the maximum thickness moved toward $x=-1$, which is again similar to that observed for the Newtonian liquids. These results imply that we are missing an important aspect of the problem in our model calculations

[1]A detailed theoretical study of the Newtonian liquids coating a vertical rotating disk will be reported elsewhere.

for the non-Newtonian liquids. Recall that ring formation was always preceded by the formation of drops that coalesce to form a ring at steady state. A lubrication approximation cannot capture such thickness variations and the full equations may need to be solved to understand the ring formation phenomenon.

Finally, we also considered if varying surface-tension effects could cause the ring formation. Since the surfactant concentration in the CTAB-NaSal solution is far above the critical micelle concentration (~ 1 mM), we expect the interface to be always saturated with the surfactant. However, Cooper-White *et al.* [9] showed that, in flows involving surface dilation, the dynamic surface tension of equimolar CTAB-NaSal solutions varying from 1 to 10 mM reduces from a value of 0.072 N/m (pure water) for surface dilation rates above 100 s^{-1} to the equilibrium value of 0.036 N/m for rates less than 1 s^{-1}, suggesting that the surface adsorption of the surfactant molecules is slow in the presence of salt. Since the maximum shear rates in our experiments are about 1 s^{-1}, it is possible that surface dilation rates of similar magnitude may result in spatial variation of surface tension and consequently influence the thickness profile. This, of course, requires solving the Stokes equation along with the appropriate interfacial boundary conditions and so is postponed to a future study.

III. CONCLUSION

In conclusion, we identify a phenomenon of ring formation when a certain class of non-Newtonian liquids coats a vertical rotating disk. Such a phenomenon is not observed for Newtonian liquids with comparable viscosities. Although, the experimental results seem to indicate that the ring formation is caused due to the shear thinning rheology of the fluids, more work is required to confirm these results.

ACKNOWLEDGMENTS

The work described in this paper was supported under the Indian Institute of Technology–Bombay seed Grant No. 03IR032. We thank Swati Prasad for performing experiments on CTAB-NaSal solution. We are in debt to Dr. T. J. Huang of National Starch Inc., USA for help with rheological measurements. N.H.P. acknowledges IIT Bombay for research assistance.

[1] R. B. Bird, R. C. Armstrong, and O. Hassager, *Dynamics of Polymeric Liquids* (Wesley, New York, 1987).
[2] F. A. Morrison, *Understanding Rheology* (Oxford University Press, New York, 2001).
[3] L. Landau and B. Levich, Acta Physicochim. URSS **17**, 42 (1942).
[4] H. K. Moffatt, J. Mec. **16**, 651 (1977).
[5] A. G. Emslie, F. T. Borron, and L. G. Peck, J. Appl. Phys. **29**, 858 (1958).
[6] S. K. Wilson, R. Hunt, and B. R. Duffy, J. Fluid Mech. **413**, 65 (2000).
[7] M. Zanfir, X. Sun, and A. Gavriilidis, Chem. Eng. Sci. **62**, 741 (2007).
[8] W.-J. Kim and S. M. Yang, J. Colloid Interface Sci. **232**, 225 (2000).
[9] J. J. Cooper-White, R. C. Crooks, and D. V. Boger, Colloids Surf., A **210**, 105 (2002).